Static One-Dimensional Distortions in Cholesteric Liquid Crystals*

H. Hervet,† J. P. Hurault, and F. Rondelez
Laboratoires d'Electronique et de Physique Appliquée, 3 av. Descartes, 94450 Limeil-Brévannes (France)
(Received 12 March 1973; revised manuscript received 26 July 1973)

We report new experimental observations on a cholesteric planar texture of pitch P and thickness L submitted to a static magnetic $\vec{H}$ or a high-frequency electric field $\vec{E}$. Two configurations are considered: (a) $\vec{H}$ parallel ω the helical axis: if $\chi_a > 0$, $L \sim P$, an array of stripes is observed at threshold. This is to be compared to the case $\chi_a > 0$, $L \gg P$, where a square gridlike pattern is nucleated in the same conditions. (b) $\vec{E}$ perpendicular to the helical axis: if $\epsilon_a < 0$, $L \gg 0$, a static array of stripes is again observed, the stripes being perpendicular to $\vec{E}$. This configuration is equivalent to the configuration $\chi_a < 0$, $\vec{H}$ perpendicular to the helical axis. The threshold conditions derived by Helfrich and Hurault in the case $L \gg P$, $\chi_a > 0$, $\vec{H}$ parallel to the helical axis seem to be also valid in those two cases. A more detailed theoretical treatment is devoted to the second geometry.

I. INTRODUCTION

The stability conditions for the cholesteric planar texture of pitch P and thickness L in a static magnetic field $\vec{H}$ have been thoroughly investigated both theoretically and experimentally.[1-9] It is then interesting to summarize what is known of this problem, depending on the field orientation with respect to the helical axis, the ratio L/P, and the sign of the molecular diamagnetic anisotropy $\chi_a = \chi_\parallel - \chi_\perp$ ($\chi_\parallel$ and $\chi_\perp$ are the susceptibility parallel and perpendicular to the local optical axis, respectively.)

Consider a thin film of cholesteric material which has been prepared in the planar texture with the helical axis perpendicular to the surfaces. Under an applied magnetic field, the molecules tend to align their long axis along certain directions, parallel to the field if χ_a is positive, perpendicular if χ_a is negative. We assume, however, that, on the walls, rigid boundary conditions pin the molecules in their original position.

A. $\vec{H}$ Perpendicular to the Helical Axis

1. $\chi_a > 0$

Under increasing fields, the cholesteric spiral is progressively untwisted up to a field H_U, where a transition to the nematic structure is observed. The theoretical predictions[1,2] have all been checked experimentally.[3-5] In that case only twist deformations are induced by the applied field.

2. $\chi_a < 0$

To the best of our knowledge, this geometry has not yet been investigated.

B. $\vec{H}$ Parallel to the Helical Axis

1. $\chi_a < 0$

The planar texture is the most stable configuration and no distortion is expected.

2. $\chi_a > 0$

Several cases are to be distinguished depending upon the ratio L/P.

(i) $L \gg P$. Helfrich[6] has predicted the onset of a periodic bending mode at a field H_H proportional to $(PL)^{-1/2}$. His predictions have been checked by Scheffer[7] and by Rondelez and Hulin.[8] At threshold, a square periodic pattern is observed. Both the threshold field and the spatial periodicity are in excellent agreement with a more recent derivation by Hurault.[9] As pointed out in Ref. 9, the threshold conditions are obtained assuming a one-dimensional distortion with a wave vector perpendicular to the cholesteric axis, without any further specification about the spatial orientation of this wave vector within the cholesteric planes. Thus, a fairly good understanding of this case seems to be presently achieved, apart from the fact that it has not been demonstrated yet why the distortion should be two-dimensional.

When the field is increased above threshold, the amplitude of the distortion increases up to a field H_B,[8] where the cholesteric planes are tilted by 90°. Above H_B the cholesteric texture is progressively unwound to the nematic state as in case A.

(ii) $L \ll P$. As in the case of the twisted nematic a transition according to Freedericksz[10] is directly observed[8] to be in good agreement with theory.[11] Above threshold, the applied field tends to achieve a complete homeotropic molecular alignment.

(iii) $L \sim P$. Apparently, much less has been said on this case. For this geometry, there is another possible deformation, as argued by Meyer.[2] Under increasing fields, a transition from the helical texture to a conical deformation might occur. The conical axis should be parallel to the field. However, the experimental observations reported so far do not seem to support this model, if we omit some preliminary results.[12]

To summarize, we can deduce from this review that two cases are worth being investigated: (i) $\vec{H}$ parallel to the cholesteric axis, $\chi_a > 0$, $L \simeq P$; (ii) $\vec{H}$ perpendicular to the cholesteric axis, $\chi_a < 0$, $L \gg P$ or $L \sim P$.

In the present paper, we report on the behavior of a planar cholesteric structure in these two geometrical configurations. As can be seen, these experiments must be performed both on a material with $\chi_a > 0$ and on a material with $\chi_a < 0$. The first class of material is easily obtained by mixing a nematic substance with a cholesteric. Moreover, the χ_a of such a mixture is generally close to the χ_a of the pure nematic, i.e., $\chi_a > 0$ and $|\chi_a| \simeq 10^{-7}$. As a result, the magnetic fields necessary to induce distortions on such a substance can be generated by using a conventional magnet.

Unfortunately, the situation is not as favorable in the case $\chi_a < 0$. Up to now, the cholesteric substances with $\chi_a < 0$ were conventional cholesteryl esters, but then $|\chi_a|$ is two orders of magnitude smaller than in the previous case, i.e., $|\chi_a| \simeq 10^{-9}$, [13] which means that much more powerful magnets are then needed.

Thus, instead of considering the case $\vec{H}$ perpendicular to the cholesteric axis, $\chi_a < 0$, we have performed our experiments on a material with $\epsilon_a < 0$ in a high-frequency ($f \simeq 10$ kHz) electric field applied perpendicular to the cholesteric axis. Indeed, we can show (see the Appendix) that in this case the onset of the distortion can be viewed as resulting from a purely dielectric effect. We insist on the fact that, generally, an applied electric field does not induce the same kind of distortions as a dc magnetic field owing to electrohydrodynamic effects. Several experiments have been described in the literature using a dc electric field. It is not always obvious that these results are not plagued by electrohydrodynamic effects due to the sample conductivity. Such effects have been demonstrated with ac electric fields [see, for instance, F. Rondelez, H. Arnould, and C. J. Gerritsma, Phys. Rev. Lett. 28, 735 (1972)]. But fortunately, in the geometrical configuration of interest and for the frequencies considered these effects can be neglected at threshold.

We shall report our observations according to the following plan: In Sec. II we discuss the details of the experimental apparatus using either an electric or a magnetic field. In Sec. III we present our results—a periodic array of stripes is optically observed at threshold for both cases under investigation. We relate the orientation of the pattern to the boundary conditions and the direction of the applied field. In Sec. IV we analyze quantitatively these one-dimensional static deformations within the framework of the theory developed by Helfrich and Hurault. Finally, we develop a detailed theoretical treatment for the geometry $\vec{H}$ (or $\vec{E}$) perpendicular to the helical axis in the Appendix.

II. EXPERIMENTAL

All our measurements are done with mixture of cholesteryl nonanoate (later referred to as CN) with *n-p* methoxy benzilidene *p-n* butyl aniline (MBBA). The mixture is mesomorphic at room temperature for all concentrations actually used. The desirable pitch for a given experiment is conveniently adjusted by varying the CN concentration. For low concentration (C between 0.1 and 5% by weight), the product PC is found to be constant.[14] At 22 °C, PC is equal to 0.12 ± 0.01 μm. The diamagnetic anisotropy χ_a of the mixture is positive and assumed to be that of undoped MBBA, $\chi_a = 1.16 \times 10^{-7}$ cgs,[15] whereas the dielectric anisotropy is negative, $\epsilon_a = -0.5$ cgs.[16]

A. Magnetic Field

For applied magnetic fields, the experimental setup has already been described elsewhere.[8] We use the usual sandwich cell with the Pyrex glass plates and Mylar spacers of variable thickness. When the measurement of the sample capacitance is needed, we use SnO_2-coated glass plates. The liquid crystal is introduced by capillarity between the two glass surfaces which have been previously rubbed according to Chatelain's technique.[17] This technique is sufficient to obtain a good planar cholesteric structure in our samples with small L/P ratios ($L/P = \frac{1}{2}$, 1, $\frac{3}{2}$). Indeed, the wall effects, which extend to about $\frac{1}{2}P$ from the surfaces, are now much more efficient in aligning the liquid crystal in the bulk than for large L/P. There is no need for a dielectric alignment[8,18] at high frequency and voltage (2 kHz, 300 V rms) to achieve a transparent disclination-free sample.

The magnetic field is applied parallel to the helical axis of the cholesteric sample held vertically into the 44-mm gap of an electromagnet with 160-mm pole pieces, which can deliver fields up to 12 kG. There is no temperature regulation and all the experiments are at room temperature, which is taken to be 22 °C. A system of totally reflecting prisms allows one to observe the sample in transmission in a direction parallel to the helical axis with a 210× polarizing microscope. The sample illumination is achieved by means of a plastic optic fiber 4 mm in diameter.

When needed, a phototransistor (Radiotechnique BP X 25) can be fixed behind the microscope eyepiece to monitor the change in transmitted light which occurs when the structure starts to distort.

To get a recording of the sample capacitance versus field, we use a 3R 116h Siemens capacitance bridge with a PAR JB5 lock-in detector. The unbalanced capacitance signal is fed to the y axis of a recorder while the x axis is driven by a Hall-effect device which gives a signal proportional to the field. To obtain uniform deformation in the liquid crystal, the scanning rate is limited to 30 G/min.

B. Electric Field

The apparatus used to apply an electric field perpendicular to the helical axis of a cholesteric with a planar texture is described in Fig. 1. It consists of two glass parallelipipeds (GP) inserted between two copper blocks (CB) and separated by tiny Mylar pieces (MYL) of 30–300 μm thickness. The copper blocks serve as electrodes and are connected to the output of a high-voltage audio-amplifier (600 V rms from 1 to 30 000 Hz for equipment designed in our laboratory, and 100 V rms from dc to 250 kHz for a Hewlett Packard 463A amplifier). This arrangement defines a small cavity of surface 15×2 mm and thickness 30–300 μm in which the liquid crystal is introduced by capillarity. Provided the two glass surfaces have been previously rubbed in parallel directions, this technique is sufficient to produce a homogeneous planar texture for the cholesteric liquid crystal after the sample has stayed unperturbed for a few hours, even for L/P values as large as 10.

The copper surfaces in contact with the liquid crystal have been heavily gold plated to minimize any electrochemical reaction. The electric field is then applied perpendicular to the helical axis and perpendicular to the molecular alignment at the glass boundaries. The field lines are believed to be uniform throughout the sample because the dielectric constant of the glass parallelipipeds has been matched with the mean dielectric constant of the liquid crystal.

An optical observation made in transmission is possible with a Leitz orthoplan polarizing microscope equipped with a 32× objective.

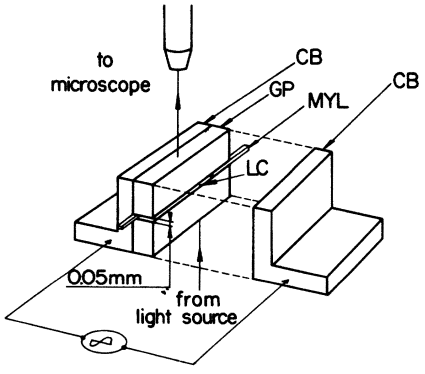

FIG. 1. Sketch of the apparatus used for applying the electric field perpendicular to the helical axis of a cholesteric planar structure. Glass parallelipipeds represented by GP, copper blocks CB, mylar spacers MYL.

III. RESULTS

A. $\vec{H}$ Parallel to the Helical Axis, $\chi_a > 0$, $L \sim P$

When H is increased slowly enough to avoid lag effects, we observe that a series of parallel straight lines appear at a field H_H, which we call the optical threshold field. Close to H_H, the lines are faint but they become more pronounced at higher fields (see Fig. 2). The lines are more easily visible between parallel polarizers but they can also be detected if they are crossed. In both cases, the distortion of the cholesteric planar structure, as determined by an abrupt change in the intensity of transmitted light, is detected at the same threshold field.

The space orientation of the lines depends on the ratio L/P and is parallel to the orientation of the molecules at the glass surfaces if $L/P = \frac{1}{2}$, perpendicular if $L/P = 1, \frac{3}{2}$. We assume here that the rubbing directions on the walls are parallel.

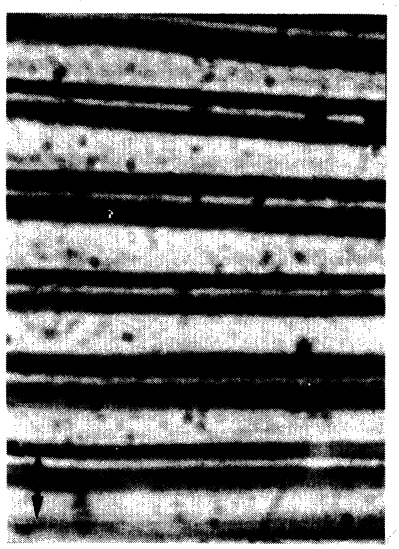

FIG. 2. Typical microscopic appearance of a periodic one-dimensional distortion in a cholesteric planar texture. $\vec{H}$ is applied parallel to the helical axis; sample thickness equals 50 μm; cholesteric pitch, 50 μm; $H = 3000$ G; the threshold is 2600 G; the wavelength of the deformation (twice the distance between two adjacent lines) is 80 μm. At threshold, the lines are only visible if the polarizers are parallel to the orientation of the molecules at the surfaces (indicated by the arrow). The lines are oriented perpendicular to the rubbing direction.

If H is still increased, the molecules tend to align along the field direction. Similar to the case $L \gg P$, we observe a 90° rotation of the helical axis at $H = H_B$. At H_B, the field is now applied perpendicular to the helix axis. For the actual values of L and P practically used, the critical field for the complete unwinding of the cholesteric spiral, H_U, is close to (or less than) H_H. So, as soon as the cholesteric is tilted, the cholesteric-nematic-field-induced transition occurs. In the so-called homeotropic geometry, birefringence effects in the narrow region where the molecular alignment changes from parallel to the glass surface to perpendicular in the bulk produce vivid colors.

When H is decreased from its maximum value, the cholesteric comes back to the original planar texture with no detectable optical effects. However, equidistant lines can sometimes appear at $H \simeq H_U$ in the case $L/P = \frac{3}{2}$: These lines are always parallel to the rubbing direction and are observed whatever the relative orientation of the polarizers may be. These properties induce us to say that what we observe then is the cholesteric tilted texture. This is quite analogous to the case $L \gg P$. That tilted structure is metastable and persists, at zero field, for about 1 min, in agreement with an extrapolation to low L/P ratios of the results obtained by Hulin[19] for the relaxation time of such a structure.

The deformations of the planar cholesteric texture can also be followed by recording the change in the sample capacitance ΔC versus the magnetic field (see Fig. 3). The dielectric constant depends on the average orientation of the molecules compared to the probing electric field used to measure the capacitance C. In the planar texture, one measures the dielectric constant perpendicular to the long molecular axis, $\epsilon_\perp$, which yields the maximum value for C, provided that $\epsilon_\perp > \epsilon_\parallel$. In the homeotropic nematic geometry one measures $\epsilon_\parallel$ and C is then minimum.

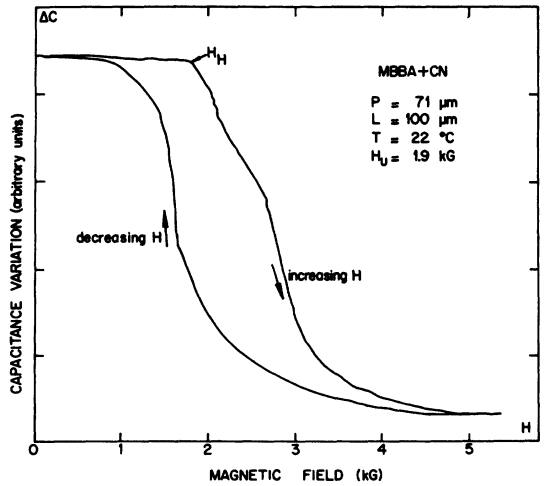

FIG. 3. Continuous recording of the sample capacitance variations with a slowly increasing applied magnetic field H. Sample thickness equals 100 μm, cholesteric pitch, 71 μm. H_U is the threshold for a cholesteric-nematic-field-induced transition as defined in Ref. 1.

Figure 3 displays the experimental curve obtained for a CN + MBBA mixture with $P = 71$ μm and $L = 100$ μm. ΔC begins to decrease at H_H. There is a steep decrease at higher fields ($H = H_B$) which corresponds to the quasisimultaneous 90° rotation of the helix and to its unwinding. Then a saturation value is reached. In decreasing H, the transition from homeotropic-nematic to the cholesteric state occurs at H_U'. As the orientation of the helical axis parallel to the glass surfaces is not energetically favorable, the system comes back immediately to the planar texture when H is further lowered and ΔC reaches its original value.

B. $\vec{E}$ Perpendicular to the Helical Axis, $\epsilon_a < 0$, $L/P \geqslant 1$

With increasing electric fields, no distortion is detected up to a field $E_\perp$, where one observes a series of straight lines equally spaced and all perpendicular to the direction of the field. $E_\perp$ is called the optical threshold. The visual appearance is very similar to the one shown in Fig. 2. These lines can only be seen if the incident polarized light is perpendicular to their orientation.

Let us recall that, when $\vec{H}$ is applied parallel to the helical axis of a cholesteric planar texture with $\chi_a > 0$, we detect[8] a gridlike pattern if $L \gg P$ or a one-dimensional array of lines if $L \sim P$. On the contrary, in the present case, an array of parallel equidistant lines is observed for all values of L/P ratios.

Within the experimental accuracy, the threshold field is independent of frequency between 1 and 250 kHz. Above threshold, the line spacing stays approximately constant up to a field E_B, where the helical axis begins to tilt along the field direction. Then the spacing decreases. For the highest available fields (3 kV/cm), the complete tilted structure was never obtained, so that the distance between two adjacent lines was always greater than $\frac{1}{2}P$. The optical pattern can now be seen for any polarization of the incident light. If the electric excitation is released, that structure is metastable and its relaxation time τ is comparable to the relaxation time of the "fingerprint" texture observed by Hulin.[19] However, τ is generally found to be shorter owing to the fact a complete tilting over was never reached.

IV. DISCUSSION

In all cases, the field-induced deformations at threshold seem to correspond to the periodic distortions predicted by Helfrich.[6] This is evidence by a parametric study of the wavelength Λ and of the threshold H_H (or $E_\perp$) as a function of L and P.

A. $\vec{H}$ Applied Parallel to Helical Axis, $\chi_a > 0$

For $\vec{H}$ applied parallel to the helical axis, $\chi_a > 0$, Hurault has derived the following formulas for H_H and Λ, the values of the magnetic field and of the spatial period at threshold, in the case $L \gg P$:

$$H_H^2 = \frac{2\pi^2}{\chi_a}(6K_2K_3)^{1/2}(PL)^{-1}, \tag{1}$$

$$\Lambda^2 = [\tfrac{3}{2}(K_3/K_2)]^{1/2}PL, \tag{2}$$

where K_2 and K_3 are the Frank elastic constants[20] for twist and bend, respectively, and are expressed in cgs units.

We have plotted in Fig. 4 the experimental values of the optical field threshold H_H vs $L^{-1/2}$ for various pitches such that $L/P = \frac{1}{2}$, 1, or $\frac{3}{2}$. Fig. 5 gives a similar plot for the period Λ at threshold. The solid lines correspond to the theoretical predictions described by Eqs. (1) and (2).

We have used a previous[8] experimental determination of K_2 and K_3, giving $K_2 = (2.2 \pm 0.7) \times 10^{-7}$ dyn at 22 °C and $K_3 = (7.45 \pm 1.1) \times 10^{-7}$ dyn. As can be seen, the agreement is still very good, although the condition $L \gg P$ is no longer fulfilled.

On the other hand, the Helfrich–Hurault model does not predict the orientation of the wave vector of the distortion with respect to the rubbing directions. Experimentally, we observe that the lines are parallel to the rubbing directions when $L/P = \frac{1}{2}$, perpendicular when $L/P = 1$ and $\frac{3}{2}$.

More generally, it seems that the orientation of the lines is fixed by the local unperturbed director right in the middle of the sample. This is demonstrated on a sample such that the molecules in the middle are at 45° from the rubbings, obtained by crossing the two rubbing directions and taking a ratio L/P equal to $\frac{5}{4}$. Then the lines are observed to be oriented at 45° from the rubbings.

B. $\vec{E}$ Perpendicular to the Helical Axis, $\epsilon_a < 0$, $L/P \geq 1$

Using the same formalism as in Ref. 9, we give, in the Appendix, a complete derivation for the case where the field is applied perpendicular to the helical axis. We find that a Helfrich–Hurault-[6,9] type infinitesimal distortion is allowed at a threshold $H_\perp$. Two equations are obtained for the values of the field $E_\perp$ (or $H_\perp$) and the spatial period $\Lambda_\perp$ at threshold. If we express our results in terms of the equivalent quantities for the case where the field is parallel to the helical axis, we get the remarkable relations

$$H_\perp = H_\parallel, \tag{3}$$

$$\Lambda_\perp = \Lambda_\parallel. \tag{4}$$

$H_\parallel$ and $\Lambda_\parallel$ are defined by Eqs. (1) and (2). Moreover, the orientation for the spatial distortion is

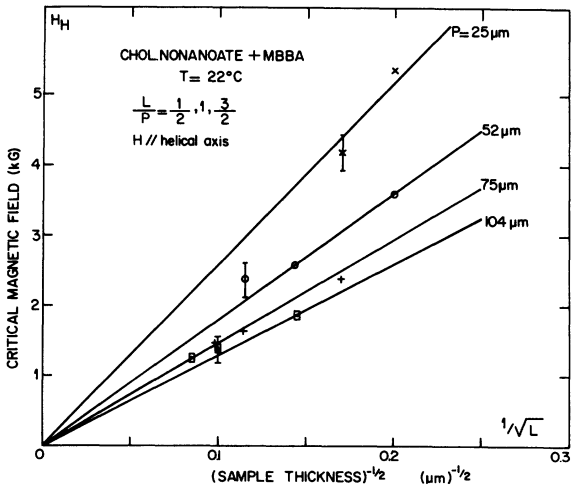

FIG. 4. Optical field threshold H_H vs $L^{-1/2}$ (L = sample thickness) for various pitches. $\vec{H}$ is parallel to the helical axis; the ratio L/P is chosen to be $\frac{1}{2}$, 1, or $\frac{3}{2}$. The solid lines correspond to the theory as described in Ref. 9.

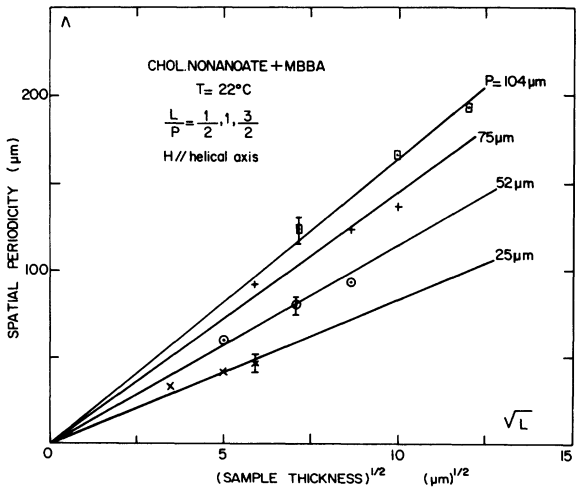

FIG. 5. Period of the deformation $\Lambda_\parallel$ observed at threshold vs $L^{1/2}$ (L = sample thickness) for various pitches. The ratio L/P is chosen to be $\frac{1}{2}$, 1, or $\frac{3}{2}$. The destabilizing magnetic field is applied parallel to the helical axis. The solid lines correspond to the theory as described in Ref. 9.

predicted to be along the field direction.

We have plotted in Fig. 6 the experimental values for the optical threshold electric field E versus $L^{-1/2}$ for various pitches. In coordinates we have indicated both the rms value of the applied electric field and the values of the equivalent magnetic field using the transformation formula

$$(|\epsilon_a|/4\pi)E_{\rm rms}^2 \longrightarrow \chi_a H^2 .$$

The solid lines correspond to a square-root dependence of the threshold versus the inverse of the sample thickness.

When the frequency of the applied electric field is varied, the threshold is found to be constant over a large range of frequencies,

$$1 < f < 250 \text{ kHz}.$$

However, an increase for the threshold value is observed at low frequencies. For our samples, of conductivity $\sigma = 10^{-9}$ $(\Omega\,\text{cm})^{-1}$, there is a 20% increase between the high-frequency (> 10 kHz) saturation value and the value at 50 Hz, probably due to electrohydrodynamic effects. At still lower frequencies, the periodic deformation is no longer nucleated.

Figure 7 gives our results for the period of the deformation versus $L^{1/2}$. The solid lines correspond to a square-root dependence of the spatial periodicity versus the sample thickness. Our experimental results fully agree with the theoretical predictions given by Eqs. (3) and (4).

From the slope of the curves displayed in Figs. 6 and 7, we can derive $K_2 = (2.2 \pm 0.7) \times 10^{-7}$ dyn at 22 °C, and $K_3 = (8.1 \pm 1.1) \times 10^{-7}$ dyn. These data are in close agreement with those previously published[8] in the case where the magnetic field is applied parallel to the helical axis.

We are then allowed to say that both the threshold field and the period for the spatial deformation are the same, within experimental errors, whenever the field is applied parallel (with $\chi_a > 0$) or perpendicular (with $\chi_a < 0$) to the helical axis $\vec{h}$. This is confirmed unambiguously by an experiment performed on a *single* sample ($\epsilon_a < 0$, $\chi_a > 0$). We record the threshold characteristics (threshold field, spatial periodicity) in the two following geometries: (i) an electric field $\vec{E}$ perpendicular to $\vec{h}$ (threshold parameters $E_\perp$ and $\Lambda_\perp$); (ii) a magnetic field $\vec{H}$ parallel to $\vec{h}$ ($H_\parallel$ and $\Lambda_\parallel$). Then, in making the equivalence H

$$H_\perp = (|\epsilon_a|/4\pi\chi_a)^{1/2} E_\perp ,$$

we find indeed, with an accuracy of 5%, that

$$H_\perp = H_\parallel , \quad \Lambda_\perp = \Lambda_\parallel .$$

V. CONCLUSIONS

The results we have reported allow us to complement our previous studies of the periodic deformations of a planar cholesteric texture in a magnetic field.

For $\vec{H}$ parallel to the helical axis, $\chi_a > 0$ and $L \sim P$, we have observed the onset of a one-dimensional array of parallel lines, in opposition to the case $L \gg P$, where a square-grid pattern was detected. These lines have various orientations compared to the rubbing directions on the walls

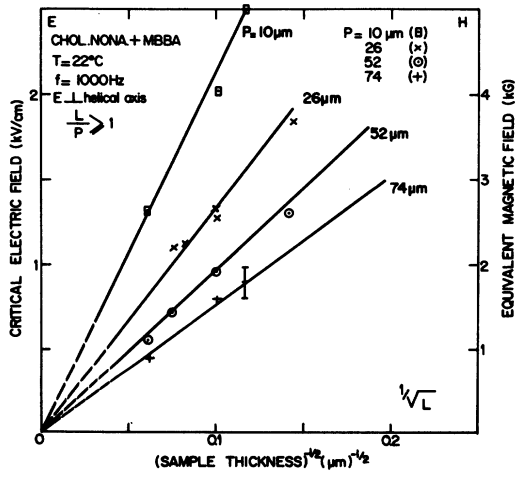

FIG. 6. Optical field threshold $E_\perp$ vs $L^{-1/2}$ (L = sample thickness) for various pitches P. The left-hand side of the ordinate axis refers to the electric field $E_\perp$ applied normal to the helical axis. The right-hand side of the ordinate axis gives the equivalent values if a magnetic field were used (see text). The solid lines correspond to the theoretical predictions as derived in the Appendix.

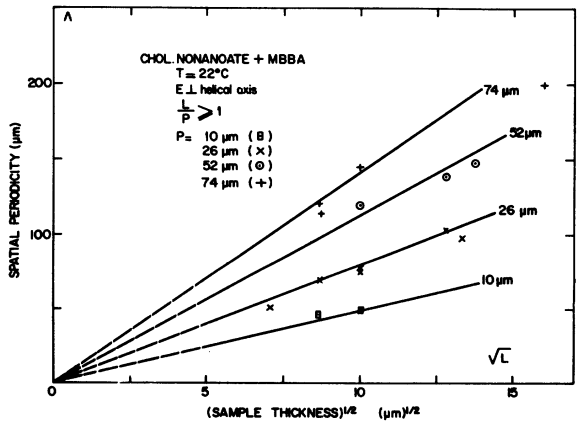

FIG. 7. Period of the deformation $\Lambda_\perp$ observed at threshold vs $L^{1/2}$ (L = sample thickness) for various pitches P. The destabilizing electric field is applied normal to the helical axis. The solid lines correspond to the theoretical predictions as derived in the Appendix.

and according to the ratio L/P. More generally, the lines seem to be perpendicular to the molecular orientation in the middle of the sample. The values of the optical threshold field and wavelength are still in quantitative agreement with the predictions of the Helfrich–Hurault model.

For $\vec{H}$ perpendicular to the helical axis, $\chi_a < 0$ (this experimental situation being simulated by a high-frequency electric field applied perpendicular to the helical axis and $\epsilon_a < 0$), the optical pattern is always a one-dimensional array of parallel equidistant lines. These lines are perpendicular to the direction of the field.

The experimental observations for threshold and spatial periodicity are in very good quantitative agreement with a theoretical model based upon a distortion "à la Helfrich" nucleated onto an already untwisted cholesteric spiral. This allows for an easy determination of the bend and twist elastic constants of the cholesteric liquid crystal.

For the sake of clarity, we have summarized in Table I the main characteristics of the various types of deformations experienced by a cholesteric planar texture in a magnetic field. From considerations of Table I, we can state that the static deformations induced by a magnetic field in a cholesteric liquid crystal seem to be presently well understood, at least at threshold. On the other hand, the theoretical descriptions of the phenomena which occur beyond threshold, such as, for example, the existence of the square-grid pattern, are still to be worked out.[21]

ACKNOWLEDGMENTS

We thank M. Courdille and P. Parquet for precious technical assistance. We gratefully acknowledge helpful discussions with Dr. E. Dubois-Violette. One of us (J.P.H.) is deeply indebted to Dr. J. M. Delrieu for critical comments on the matter presented in the Appendix.

APPENDIX

In this appendix, we give a microscopic theoretical derivation of the threshold conditions for a cholesteric structure with $\chi_a < 0$ in a magnetic field $\vec{H}$ applied perpendicular to the cholesteric axis. For this purpose, we proceed in a way very similar to Ref. 9: We see whether an infinitesimal distortion "à la Helfrich" can be nucleated, i.e., under what field this distortion is compatible with the stability conditions. However, compare to the case $\chi_a > 0$, $\vec{H}$ applied parallel to the helical axis, we have to be more cautious. Indeed, in this former case, we considered the distortion to be nucleated on a completely unperturbed planar

TABLE I. Deformations induced by a static magnetic field in cholesteric liquid crystals with a planar texture.

Diamagnetic anisotropy	$\chi_a > 0$		$\chi_a < 0$	
Field orientation compared to the unperturbed helical axis	Parallel	Perpendicular	Parallel	Perpendicular
Nature of instability	Periodic bend and twist modes[a]	Chol. → nematic transition[b]	Stable	Periodic bend and twist modes[c]
Threshold	$H_{H\parallel}$	H_U	...	$H_H, \perp$
Characteristic length	$\Lambda_\parallel$	$P(H)$ $P \to \infty$ for $H \to H_U$	...	$\Lambda_\perp$
Optical pattern	Square grid if $L \gg P$ Periodic stripes if $L \sim P$ No pattern if $L \ll P$	No pattern except in a Canowedge geometry[d]		Periodic stripes
Orientation of the pattern at threshold	Lines parallel and/or perpendicular to the local optical axis in the middle of the sample			Lines perpendicular to the field
Agreement with theory for H and Λ	Quantitative[c,e,f]	Quantitative[d]	...	Quantitative[c]
Behavior above threshold	90° rotation[f] and chol. → nematic transition for $L \gtrsim P$	...	...	90° rotation

[a] W. Helfrich, Ref. 6, and J. P. Hurault, Ref. 9.
[b] P. G. de Gennes, Ref. 1, and R. B. Meyer, Ref. 2.
[c] Present work.
[d] G. Durand, L. Léger, F. Rondelez, and M. Veyssié, Ref. 4.
[e] T. J. Scheffer, Ref. 7.
[f] F. Rondelez and J. P. Hulin, Ref. 8.

texture. On the contrary, in the present case, applying a finite field perpendicular to the cholesteric axis induces a finite untwisting of the helix,[1,2] i.e., the distortion "à la Helfrich" is nucleated onto a perturbed cholesteric texture.

Let us now consider a cholesteric texture sandwiched between the planes $z = +\frac{1}{2}L$ and $z = -\frac{1}{2}L$. At rest, the coordinates of the director are

$$n_x = \cos\psi_0, \quad n_y = \sin\psi_0, \quad n_z = 0, \tag{A1}$$

with

$$\psi_0 = t_0 z, \tag{A2}$$

t_0 being such that

$$t_0 = 2\pi/P. \tag{A3}$$

For the most general type of perturbation, the coordinates of the director are given by

$$n_x = \cos\Phi\cos\Theta, \quad n_y = \sin\Phi\cos\Theta, \quad n_z = \sin\Theta. \tag{A4}$$

Now, we assume that our distortion depends only on two coordinates, z and x, Ox being an arbitrary axis parallel to the cholesteric layers. If we recall that we consider an infinitesimal distortion, it will be sufficient to expand the Frank elastic energy and the magnetic energy up to terms of second order in Θ, its derivatives, and $\partial\Phi/\partial x$. Thus, the elastic contribution G_e to the Gibbs energy can be written as

$$G_e = \tfrac{1}{2}\int d^3r\Big\{K_1\Big(-\frac{\partial\Phi}{\partial x}\sin\Phi + \frac{\partial\Theta}{\partial z}\Big)^2 + K_2\Big(t_0 - \frac{\partial\Phi}{\partial z}\cos^2\Theta - \frac{\partial\Theta}{\partial x}\sin\Phi + \Theta\frac{\partial\Phi}{\partial x}\cos\Phi\Big)^2$$
$$+ K_3\Big[\Big(\Theta\sin\Phi\frac{\partial\Phi}{\partial z} + \frac{1}{2}\frac{\partial\Phi}{\partial x}\sin 2\Phi\Big)^2 + \Big(\frac{\partial\Phi}{\partial x}\cos^2\Phi + \Theta\frac{\partial\Phi}{\partial z}\cos\Phi\Big)^2 + \Big(\frac{\partial\Theta}{\partial x}\cos\Phi\Big)^2\Big]\Big\}, \tag{A5}$$

where K_1, K_2, and K_3 denote the Frank elastic constants for splay, twist, and bend, respectively.

If the direction of the applied magnetic field $\vec{H}$ makes an angle Ω with the Ox axis, the magnetic contribution G_m to the Gibbs energy can be written as

$$G_m = -\tfrac{1}{2}\int \chi_a H^2 \cos^2\Phi'\cos^2\Theta, \tag{A6}$$

where

$$\Phi' = \Phi - \Omega. \tag{A7}$$

The stability conditions are obtained by writing that the local derivatives with respect to the total Gibbs energy with respect to Θ and Φ are equal to zero, or

$$\frac{\delta G_e}{\delta\Phi}(\vec{r}) + \frac{\delta G_m}{\delta\Phi}(\vec{r}) = 0, \tag{A8}$$

$$\frac{\delta G_0}{\delta\Theta}(\vec{r}) + \frac{\delta G_m}{\delta\Theta}(\vec{r}) = 0. \tag{A9}$$

Thus, we first compute these four local derivatives and express them in terms of the following new variables: θ, φ, ψ, and t, where φ is the infinitesimal deviation of the twist angle associated with the distortion "à la Helfrich." Thus

$$\Theta = \theta\cos\psi,$$
$$\Phi = \psi + \varphi, \quad \psi' = \psi - \Omega, \tag{A10}$$
$$t = \frac{\partial\psi}{\partial z}.$$

The expressions for our local derivatives are then given by

$$\frac{\delta G_e}{\delta\Phi} = -(K_1\sin^2\psi + K_3\cos^2\psi)\Big(\frac{\partial^2\varphi}{\partial x^2} + t\frac{\partial\theta}{\partial x}\Big) - K_2\Big(\frac{\partial^2\psi}{\partial z^2} + \frac{\partial^2\varphi}{\partial z^2} + t\cos 2\psi\frac{\partial\theta}{\partial x}\Big)$$
$$+ \tfrac{1}{2}(K_1 - K_2)\sin 2\psi\frac{\partial^2\theta}{\partial x\partial z} - 2K_2(t_0 - t)\cos^2\psi\frac{\partial\theta}{\partial x}, \tag{A11}$$

$$\frac{\delta G_m}{\delta\Phi} = \tfrac{1}{2}\chi_a H^2\sin 2\psi' + \varphi\chi_a H^2\cos 2\psi', \tag{A12}$$

$$\frac{\delta G_e}{\delta\Theta}\cos\theta = t\Big(t\theta + \frac{\partial\varphi}{\partial x}\Big)(K_1 + K_3)\cos^2\psi - K_3\cos^4\psi\frac{\partial^2\theta}{\partial x^2} - \tfrac{1}{4}K_2\sin^2 2\psi\frac{\partial^2\theta}{\partial x^2} - \tfrac{1}{2}(K_2 - K_1)\sin 2\psi\frac{\partial^2\varphi}{\partial x\partial z}$$
$$+ K_1 t\sin 2\psi\frac{\partial\theta}{\partial z} - K_1\cos^2\psi\frac{\partial^2\theta}{\partial z^2} + K_1\frac{\partial t}{\partial z}(\tfrac{1}{2}\sin 2\psi)\theta - 2K_2\cos^2\psi(t_0 - t)K_2\Big(t\theta + \frac{\partial\varphi}{\partial x}\Big), \tag{A13}$$

$$\frac{\delta G_m}{\delta \Theta}\cos\theta = \tfrac{1}{2}\theta\chi_a H^2\cos^2\psi'\cos^2\psi. \tag{A14}$$

From (A8), (A11), and (A12), we notice that the zeroth-order terms must cancel out in (A8). Therefore we must have

$$K_2\frac{\partial^2\psi}{\partial z^2} = \tfrac{1}{2}\chi_a H^2\sin 2\psi'. \tag{A15}$$

We *assume* now that $L \gg P$, and that the threshold field is much lower than the untwisting field. Therefore, we may write (which we can verify *a posteriori*) from (A13), (A3), and (A8),

$$t \simeq t_0 - \frac{\chi_a H^2}{4K_2 t_0}\cos 2\psi', \tag{A16}$$

$$\frac{\partial t}{\partial z} \simeq \frac{\chi_a H^2}{2K_2}\sin 2\psi'.$$

We can then inject (A16) into (A11), (A12), (A13), and (A14). From now on, we proceed *exactly* in the same manner as in Ref. 9. In order to solve the stability conditions, taking into account Eqs. (A11)–(A14) plus the boundary conditions $\theta = \varphi = 0$ for $Z = \pm\frac{1}{2}L$, we must expand θ and φ in series of harmonics of 2ψ. However, when $L \gg P$, it is easily demonstrated that these expansions can be limited to

$$\varphi = (\varphi_0 + \varphi_1\cos 2\psi)\cos qz\cos kx, \tag{A17}$$

$$\theta = \theta_0\cos qz\sin kx, \tag{A18}$$

where k denotes the magnitude of the wave vector of our distortion, q being such that

$$q = \pm\pi/L. \tag{A19}$$

Using (A17) and (A18), together with (A16), in relations (A11)–(A14), the stability conditions (A8) and (A9) yield three homogeneous relations between φ_0, φ_1, and θ, where the negligible corrections are omitted (which we check *a posteriori*):

$$\tfrac{1}{2}(K_3+K_1)(k^2\varphi_0 - t_0 k\theta_0) + K_2 q^2\theta_0 + \tfrac{1}{4}(K_3-K_1)k^2\theta_1 - \frac{K_3-K_1}{16K_2}\frac{k}{t_0}\chi_a H^2\cos 2\Omega\theta_0 = 0, \tag{A20}$$

$$\chi_a H^2\cos 2\Omega\varphi_0 + \tfrac{1}{2}(K_3-K_1)(k^2\varphi_0 - t_0 k\theta_0) + K_2(4t_0^2\varphi_1 - t_0 k\theta_0) + \tfrac{1}{2}(K_3+K_1)k^2\varphi_1 - \frac{\chi_a H^2}{4K_2 t_0}\cos 2\Omega[\tfrac{1}{2}(K_3+K_1)+K_2]k\theta_0 = 0, \tag{A21}$$

$$\tfrac{1}{4}\chi_a H^2(1+\tfrac{1}{2}\cos 2\Omega)\theta_0 + \tfrac{1}{2}(K_3+K_1)t_0(t_0\theta_0 - k\varphi_0) + \tfrac{1}{8}(3K_3+K_2)k^2\theta_0 - \tfrac{1}{4}(2K_2+K_3-K_1)t_0 k\varphi_1 - \tfrac{1}{16}(\chi_a H^2\cos 2\Omega)\frac{K_3-K_1}{K_2}\theta_0 = 0. \tag{A22}$$

These last three conditions are found compatible if

$$\tfrac{1}{4}\chi_a H^2(1+\cos 2\Omega) + \frac{K_2 q^2 t_0^2}{k_2} + \tfrac{3}{8}K_3 k^2 = 0. \tag{A23}$$

From (A23), we see that, provided that χ_a is negative, a distortion "à la Helfrich" with a wave vector k can be nucleated at a field H given by (A23). Of all threshold fields, the minimum one, $H_\perp$, is obtained for $\Omega = 0$, i.e., for $\vec{k}$ aligned along the field (the resulting fringes being normal to the field) and for k such that

$$k^2 = k_\perp^2 = (8K_2/3K_3)^{1/2}t_0 q, \tag{A24}$$

$H_\perp$ being such that

$$H_\perp^2 = -(1/\chi_a)(6K_2K_3)^{1/2}t_0 q. \tag{A25}$$

Therefore, if $H_\parallel$ and $k_\parallel$ denote the values of the field and wave vector at the onset of a similar distortion when the field is applied parallel to the helical axis of a material with $\chi_a = |\chi_a|$, we have the remarkable relations

$$k_\perp \equiv k_\parallel, \qquad H_\perp \equiv H_\parallel. \tag{A26}$$

Moreover, as Helfrich points it out in Ref. 6, the direction of $\vec{k}$ is unambiguously determined in the "perpendicular" geometry, which is not the case in the "parallel" geometry.

Finally it remains to be shown that the same kind of distortion can be obtained with a high-frequency electric field $E\cos\omega t$ applied perpendicular to the helical axis with $\epsilon_a < 0$. Indeed, the calculation of the dielectric couples goes along the same way as the calculation of the magnetic couples. On the other hand, space charges might be formed and give rise to complications. However, such effects will be negligible when the frequency of the exciting field is much higher than the frequency of relaxation of the space charges. In this high-frequency limit, the threshold field (for $\epsilon_a < 0$) is given by

$$-(\epsilon_a/4\pi)\tfrac{1}{2}E_{\rm th}^2 = (6K_2K_3)^{1/2}t_0 q. \tag{A27}$$

*Supported by D.R.M.E. under Contract No. 72-34-208.
†Permanent address: College de France, Physique de la matière condensée, Place Marcelin Berthelot, Paris Vème.
[1]P. G. de Gennes, Solid State Commun. 6, 163 (1968).
[2]R. B. Meyer, Appl. Phys. Lett. 12, 281 (1968).
[3]E. Sackmann, S. Meiboom, and L. C. Snyder, J. Am. Chem. Soc. 89, 5981 (1967).
[4]G. Durand, L. Léger, F. Rondelez, and M. Veyssie, Phys. Rev. Lett. 22, 227 (1969).
[5]R. B. Meyer, Appl. Phys. Lett. 14, 208 (1969).
[6]W. Helfrich, Appl. Phys. Lett. 17, 531 (1970).
[7]T. J. Scheffer, Phys. Rev. Lett. 28, 593 (1972).
[8]F. Rondelez and J. P. Hulin, Solid State Commun. 10, 1009 (1972).
[9]J. P. Hurault, J. Chem. Phys. (to be published).
[10]V. Freedericksz and V. Zolina, Z. Kristallogr. 79, 225 (1931).
[11]A. Rapini, thesis (University of Orsay, 1970) (unpublished).
[12]H. Baessler, T. M. Laronge, and M. M. Labes, J. Chem. Phys. 51, 3213 (1969).
[13]T. M. Laronge, H. Baessler, and M. M. Labes, J. Chem. Phys. 51, 4186 (1969).
[14]R. Cano, C. R. Acad. Sci. (Paris) 251, 1139 (1960).
[15]H. Gasparoux, B. Regaya, and J. Prost, C. R. Acad. Sci. B 272, 1168 (1971).
[16]D. Diguet, F. Rondelez, and G. Durand, C. R. Acad. Sci. B 271, 954 (1970).
[17]P. Chatelain, Bull. Soc. Fr. Mineral. 60, 300 (1937).
[18]W. Haas, J. Adams, and J. B. Flannery, Phys. Rev. Lett. 24, 577 (1970).
[19]J. P. Hulin, Appl. Phys. Lett. 10, 455 (1972).
[20]F. C. Frank, Discuss. Faraday Soc. 25, 19 (1958).
[21]J. M. Delrieu (unpublished).

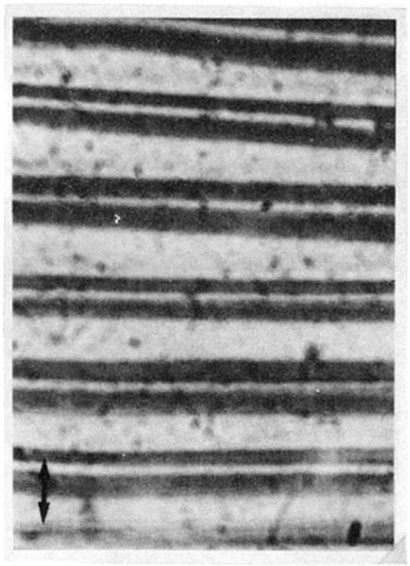

FIG. 2. Typical microscopic appearance of a periodic one-dimensional distortion in a cholesteric planar texture. $\vec{H}$ is applied parallel to the helical axis; sample thickness equals 50 μm; cholesteric pitch, 50 μm; $H=3000$ G; the threshold is 2600 G; the wavelength of the deformation (twice the distance between two adjacent lines) is 80 μm. At threshold, the lines are only visible if the polarizers are parallel to the orientation of the molecules at the surfaces (indicated by the arrow). The lines are oriented perpendicular to the rubbing direction.